

# Frictionally Excited Thermoelastic Instability in Multi-Disk Clutches and Brakes

**P. Decuzzi**

e-mail: p.decuzzi@dimeng.poliba.it  
Dipartimento di Progettazione e Produzione Industriale,  
Politecnico di Bari, V. Japigia 182,  
70126 Bari, Italy

**M. Ciaverella**

CNR-IRIS (Consiglio Nazionale delle Ricerche),  
Computational Mechanics of Solids (COMES),  
Str. Crocefisso 2/B, 70125 Basri, Italy

**G. Monno**

Dipartimento di Progettazione e Produzione Industriale,  
Politecnico di Bari, V. Japigia 182,  
70126 Bari, Italy

*The propensity toward thermoelastic instability (TEI) in multi-disk clutches and brakes is investigated by introducing a new bidimensional analytical model, where metal and friction disks are replaced by two-dimensional layers of finite thickness. This new model permits to estimate the effect of the thickness ratio  $a_1/a_2$ , between friction and metal disks, on the critical speed, critical wave parameter and migration speed of the sliding system. It is found that as the thickness ratio  $a_1/a_2$  decreases the critical speed reduces significantly taking up values about 80 percent smaller than that predicted by previous two-dimensional models for commonly used ratios ( $0.1 < a_1/a_2 < 1$ ), whilst the critical wave parameter slightly increases. Therefore, not only the susceptibility towards TEI can be reduced by changing the material properties of the friction lining but also by adjusting suitably the thickness ratio of the disks. The two-dimensional model is also employed to determine the critical speed in a real multi-disk clutch, and the results are compared with a three-dimensional finite element code. It is shown that the critical speed estimated by the present two-dimensional plane strain model is in good agreement with that determined by the FE code for sufficiently large radial thickness of the disks, whilst the two-dimensional plane stress solution has to be used for relatively small radial thickness ratios. Also, it is found that the critical number of hot spots is independent of the radial thickness ratio and it is correctly predicted by the two-dimensional model.*

[DOI: 10.1115/1.1352740]

## 1 Introduction

The *hot spotting* phenomenon can be experienced by clutches and brakes and is responsible for load concentration over small zones of high pressure and temperature (*hot spots*). At an unaided eye, such hot spots appear as oval, bluish and equally spaced stains which are arranged antisymmetrically on each side of the metal disks. A metallographic investigation reveals that such stains result from deposits of decomposed oil and degraded friction material. Hot spotting has been attributed to the phenomenon of *thermoelastic instability (TEI)* by Barber [1], who firstly studied it in railway braking application. Recently, the introduction of new asbestos free friction materials and the growing demand for higher performances have increased the propensity of brakes and clutches towards thermoelastic instability [2]. It is extensively reported in the literature that high mechanical and thermal loads strongly affect durability and performance of friction linings. For instance, Yang et al. [3], performing thermal gravimetric analysis on a multi-disk wet paper clutch, have shown that cellulose components are completely degraded for temperature higher than 400°C. Also, Takezaki and Kubota [4], investigating the effect of non-uniform contact pressure in clutches, measured a decrease in average friction coefficient of about 20 percent, an increase in carbonization and wear of the friction material respectively of about 500 percent and 400 percent, just after 1000 engagement cycles.

The susceptibility toward hot spots formation depends on the relative speed, geometry and material properties of the sliding system. By means of a perturbation analysis, Burton and coworkers [5] showed that there exists a sliding speed below which the system is unconditionally stable, whilst for larger speeds even a small perturbation grows leading to fully developed hot spots in a very short time. Burton's analysis modeled seal-like configurations as two sliding half-planes, and its application to actual

clutches and brakes overestimates significantly the critical speed. Clearly, the main approximation relies on the non finite dimensions of the sliding bodies. Lee and Barber [6] introduced a model where a thin metal disk slides between two friction half-planes, obtaining more reasonable results but still the critical speed is overestimated, as shown in the sequel. Obviously only a finite element model can take account of the actual geometry of the sliding system: axialsymmetry, finite axial and radial thickness of the disks. This way has been followed, for instance, by Zagrodzki [7], who solved the transient coupled thermoelastic problem for a real 9 disk clutch, showing that an uneven pressure distribution over an ending plate can grow in time, leading also to uneven temperature distribution, over all the disks. Despite their flexibility and accuracy, finite element modeling of thermoelastic problems is extremely computer intense. Only recently Yi et al. [8], introduced a reasonably efficient finite element model for a multi-disk clutch or brake. In particular, they showed that, as the number of disks increases, the critical speed reduces approaching a fixed minimum value for just 9 disks, and that the three-dimensional solution is bracketed between the two-dimensional plane strain and plane stress solution. Consequently, the critical speed of real clutches or brakes with 9 or more disks, commonly used in aircrafts and high speed railway applications, can be estimated referring to virtual two-dimensional clutches or brakes with an infinite number of disks.

In this paper, the propensity toward thermoelastic instability of a two-dimensional model of a clutch/brake, with an infinite number of disks, is studied, under both plane strain and plane stress assumptions. This model is used to investigate the influence of the disk thickness ratio on the critical speed, critical wave parameter and migration speed of the system. Different modes of deformation for friction and metal disks are investigated. Subsequently, the two-dimensional model is applied to a real multi-disk clutch and the results are compared with a three-dimensional axisymmetric finite element solution.

Contributed by the Tribology Division for publication in the ASME JOURNAL OF TRIBOLOGY. Manuscript received by the Tribology Division April 6, 2000; revised manuscript received December 7, 2000. Associate Editor: B. O. Jacobson.

## 2 Formulation

A pack containing an infinite series of two-dimensional metal and friction layers is considered (Fig. 1). Such a system is symmetric about the mid planes of each layer, thus the analysis can be restricted to a mid friction layer (1) sliding with relative speed  $V$  over a mid metal layer (2), with suitable boundary conditions prescribed over the planes of symmetry, as discussed later on.

As a consequence of the frictional heat generated at the contact interface, the temperature of the sliding disks increases tending to a steady state value depending on the thermomechanical boundary conditions. In order to assess the susceptibility toward hot spotting, that is to assess the thermoelastic stability of the system, this steady state solution is perturbed superimposing a non-uniform contact pressure. Thus, the perturbed solution has to satisfy the thermomechanical governing equations and the associated homogeneous boundary value problem.

In real systems, several factors can produce non uniform contact pressure such as thickness variation and lack of parallelism of the disks, non adequate constraining of the ending plates and eventually mechanical vibrations transmitted from the engine or the road to the clutch/brake. Noting that a sufficiently regular perturbation can be expanded in Fourier series and, as long as it remains small, each term of the series can be considered independently, the system is driven unstable if at least one component of the series grows in time. Therefore, without losing generality, we consider a contact pressure perturbation of the form

$$p(x;t) = p_0 e^{bt} e^{jmx}, \quad (1)$$

where the growth rate  $b$  can be (i) negative—stable perturbation, (ii) positive—unstable perturbation, as well as (iii) zero—threshold of instability, for which the critical speed  $V_{cr}$  is determined.

Geometrical symmetry does not imply load and displacement symmetry. In fact, numerical analysis of multi-disk clutches and brakes [7] showed that metal disks are likely to deform antisymmetrically (*asym*), whilst friction disks exhibit symmetric deformations (*sym*). However, in the present paper four different sets of boundary conditions are investigated, namely *sym*<sub>1</sub>–*sym*<sub>2</sub>; *sym*<sub>1</sub>–*asym*<sub>2</sub>; *asym*<sub>1</sub>–*sym*<sub>2</sub> and *asym*<sub>1</sub>–*asym*<sub>2</sub>, with the scope of determining the most critical set of boundary conditions.

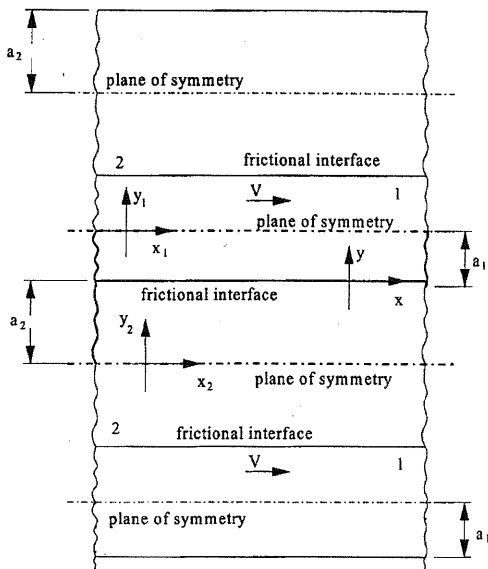


Fig. 1 An infinite pack of friction (1) and metal (2) layers sliding with a relative speed  $V$

In general, the disturbance could be not stationary with respect to the layers. Thus, a migration speed  $c_i = c - V_i$  is introduced and defined as the relative speed of the disturbance with respect to the layer  $i$ . The absolute speed of the disturbance is denoted by  $c$ . Two frames of reference  $(x_1, y_1)$  and  $(x_2, y_2)$  are considered fixed over the two layers and with center on the mid planes, whilst a third frame  $(x, y)$  moves with the perturbation (Fig. 1). Therefore, it follows that

$$x = x_i - c_i t; \quad y = y_i + (-1)^i a_i \quad (2)$$

and

$$V = c_1 - c_2, \quad (3)$$

where positive speeds are directed as the  $x$ -axis.

The following formulation is a generalization of that of Lee and Barber [6]. Firstly, the perturbed temperature field is evaluated by solving the transient Fourier's equation. Subsequently, the thermoelastic problem is solved by superimposing a suitable solution of the isothermal elastic problem on a particular solution of the equation of thermoelasticity.

**2.1 Temperature Field.** The temperature distribution in both bodies is governed by the Fourier's equation

$$\frac{\partial^2 T_i}{\partial x_i^2} + \frac{\partial^2 T_i}{\partial y_i^2} = \frac{1}{k_i} \frac{\partial T_i}{\partial t}, \quad (4)$$

where  $k_i = K_i / (\rho_i c_{pi})$  is the coefficient of diffusivity with  $K_i$ ,  $\rho_i$ , and  $c_{pi}$  the conductivity, the density and specific heat of the material  $i$ , respectively. A suitable solution of Eq. (4) is given by

$$T_i(x_i, y_i; t) = (A_i e^{+\lambda_i y_i} + B_i e^{-\lambda_i y_i}) e^{bt} e^{jm(x_i - c_i t)} \quad (5)$$

with

$$\lambda_i = \xi_i + j \eta_i = \sqrt{\left(m^2 + \frac{b}{k_i}\right) - j \left(\frac{mc_i}{k_i}\right)}. \quad (6)$$

The four constants  $A_i$  and  $B_i$  are determined by satisfying the homogeneous thermal boundary conditions associated with the perturbation problem. Therefore, for a *symmetric layer*, the heat flux across the plane of geometric symmetry is null

$$q_{y_i}|_{y_i=0} = -K_i \frac{\partial T_i}{\partial y_i} \Big|_{y_i=0} = 0; \quad \text{sym} \quad (7)$$

On the other hand, for an *antisymmetric layer*, the temperature over the plane of symmetry must be null, giving

$$T_i|_{y_i=0} = 0; \quad \text{asym} \quad (8)$$

Also, by imposing perfect contact at the friction interface, the surface temperature of both bodies must be identical, hence,

$$T_1|_{y=0} = T_o = T_2|_{y=0}.$$

After few algebraic manipulations and considering the first of (2), it follows that

$$T_i(x, y_i; t) = T_o \frac{g[(-1)^i \lambda_i y_i]}{g(\lambda_i a_i)} e^{bt + jmx}, \quad (9)$$

where  $g(\cdot) = \cosh$  for symmetrical and  $g(\cdot) = \sinh$  for antisymmetrical boundary conditions. The fourth thermal boundary condition is considered later on.

**2.1 Thermoelastic Stresses and Displacements.** The particular solution of the thermoelastic problem is given in form of a strain potential  $\psi$  [6] that must satisfy the equation

$$\nabla^2 \psi_i = \frac{2\mu_i \alpha_i (1 + \nu_i)}{1 - \nu_i} T_i, \quad (10)$$

where  $\mu_i = E_i / [2(1 + \nu_i)]$  is the shear modulus,  $\alpha_i$  the coefficient of thermal expansion, and  $\nu_i$  the Poisson's ratio. The corresponding displacement and stress field components are given by

$$\begin{aligned} u_{x_i} &= \frac{1}{2\mu_i} \frac{\partial \psi_i}{\partial x}; & u_{y_i} &= \frac{1}{2\mu_i} \frac{\partial \psi_i}{\partial y}; \\ \sigma_{yy_i} &= -\frac{\partial^2 \psi_i}{\partial x^2}; & \sigma_{xy_i} &= \frac{\partial^2 \psi_i}{\partial x \partial y}. \end{aligned} \quad (11)$$

The strain potential introduced by Lee and Barber [6] is given by

$$\psi_i = \frac{\beta_i T_o}{\lambda_i^2 - m^2} \left[ \frac{g(\lambda_i y_i)}{g(\lambda_i a_i)} \right] e^{bt+jmx}, \quad (12)$$

which is singular if  $\lambda_i = m$ , that is if the migration speed  $c_i$  goes to zero. In this paper, a different strain potential is proposed in order to avoid singularity, that is

$$\psi_i = \frac{\beta_i T_o}{\lambda_i^2 - m^2} \left[ \frac{g(\lambda_i y_i)}{g(\lambda_i a_i)} - \frac{g(my_i)}{g(ma_i)} \right] e^{bt+jmx}, \quad (13)$$

which still satisfies Eq. (10). For  $\lambda_i \rightarrow m$ , expanding the term  $g(\lambda_i y_i)/g(\lambda_i a_i)$  in Taylor series of initial point  $m$ , and substituting it back in (13), it follows that

$$\psi_i = \frac{\beta_i T_o}{\lambda_i + m} \frac{\partial}{\partial \lambda_i} \left[ \frac{g(\lambda_i y_i)}{g(\lambda_i a_i)} \right]_{\lambda_i=m} e^{bt+jmx}, \quad c_i = 0, \quad (14)$$

where the singular term ( $\lambda_i \rightarrow m$ ) has been canceled out.

A general solution to the isothermal elastic problem is given by superposing solutions  $A$  and  $D$  of Green and Zerna ([9], 5.6), where the displacement and stress field components are given in terms of harmonic potential functions  $\phi_i$  and  $\omega_i$  ( $\nabla^2(\phi_i, \omega_i) = 0$ )

$$\begin{aligned} u_{x_i} &= \frac{1}{2\mu_i} \frac{\partial \phi_i}{\partial x} + \frac{1}{2\mu_i} y_i \frac{\partial \omega_i}{\partial x} \\ u_{y_i} &= \frac{1}{2\mu_i} \frac{\partial \phi_i}{\partial y} + \frac{1}{2\mu_i} y_i \frac{\partial \omega_i}{\partial y} - \frac{3-4\nu_i}{2\mu_i} \omega_i \\ \sigma_{xx_i} &= \frac{\partial^2 \phi_i}{\partial x^2} + y_i \frac{\partial^2 \omega_i}{\partial x^2} - 2\nu_i \frac{\partial \omega_i}{\partial y} \\ \sigma_{yy_i} &= -\frac{\partial^2 \phi_i}{\partial x^2} + y_i \frac{\partial^2 \omega_i}{\partial y^2} - 2(1-\nu_i) \frac{\partial \omega_i}{\partial y} \\ \sigma_{xy_i} &= \frac{\partial^2 \phi_i}{\partial x \partial y} + y_i \frac{\partial^2 \omega_i}{\partial x \partial y} - (1-2\nu_i) \frac{\partial \omega_i}{\partial x}. \end{aligned} \quad (15)$$

It is easily verified by back substitution that

$$\phi_i = C_i \frac{g(my_i)}{g(ma_i)} e^{jmx}; \quad \omega_i = D_i \frac{g'(my_i)}{g'(ma_i)} e^{jmx}, \quad (16)$$

where prime denotes differentiation. Notice that for a *symmetrical layer*

$$u_{y_i} = 0; \quad \sigma_{xy_i} = 0 \quad \text{sym}$$

on the mid plane; whilst for a *antisymmetric layer*

$$u_{x_i} = 0; \quad \sigma_{yy_i} = 0 \quad \text{asym.}$$

The four constants  $C_i$  and  $D_i$  are determined by imposing mechanical contact conditions on the friction surface ( $y=0$ ), thus

$$\begin{aligned} u_{y1} - u_{y2} &= 0 \\ \sigma_{yy1} - \sigma_{yy2} &= 0 \\ \sigma_{xy1} - \sigma_{xy2} &= 0 \\ \sigma_{xy1} + f\sigma_{yy1} &= 0. \end{aligned} \quad (17)$$

Finally, the contact pressure is given by

$$p = p_o e^{bt} e^{jmx} = -\sigma_{yy1}. \quad (18)$$

**2.3 The Characteristic Equation.** The fourth thermal boundary condition states that the heat flux generated at the friction interface has to balance the mechanical power lost due to friction, that is

$$q_{y1} - q_{y2} = -K_1 \frac{\partial T_1}{\partial y} \Big|_{y=0} + K_2 \frac{\partial T_2}{\partial y} \Big|_{y=0} = fVp. \quad (19)$$

Substituting the results given in the previous paragraphs into Eq. (19) and setting the growth rate  $b$  to zero, since we are only interested into the threshold of instability, the following non-linear equation with complex terms holds

$$\left\{ K_1 \lambda_1 \frac{g'_1(\lambda_1 a_1)}{g_1(\lambda_1 a_1)} + K_2 \lambda_2 \frac{g'_2(\lambda_2 a_2)}{g_2(\lambda_2 a_2)} \right\} T_o - fVp_o = 0, \quad (20)$$

where  $V = V_{cr}$ . In the special case of *sym1 - asym2*, the above equation takes the form

$$\{K_1 \lambda_1 \tan h(\lambda_1 a_1) + K_2 \lambda_2 \cot h(\lambda_2 a_2)\} T_o - fV_{cr} p_o = 0, \quad (21)$$

which tends to that given by Lee and Barber [6] for antisymmetric mode, as  $a_1$  goes to infinity.

Finally, fixing the materials properties, the thicknesses ratio  $a_1/a_2$  and the wave number  $m$  of the assumed perturbation, the real and imaginary part of Eq. (20), together with the kinematic condition  $V = c_1 - c_2$ , give a non-linear system of three equations in the three unknowns  $V$ ,  $c_1$ , and  $c_2$ .

The present formulation is for plane stress assumption. The plane stress solution is obtained by introducing the following fictitious material constants

$$E' = E \frac{(1+2\nu)}{(1+\nu)^2}; \quad \nu' = \frac{\nu}{(1+\nu)}; \quad \alpha' = \alpha \frac{(1+\nu)}{(1+2\nu)}. \quad (22)$$

**2.4 The Numerical Code.** The whole procedure so far described has been implemented in *Mathematica* [10], in order to perform automatically lengthy symbolic calculations. The procedure is briefly described in the sequel for the case of symmetric friction layers (1) rubbing over antisymmetric metal layers (2). In this case, the strain potentials given in Eq. (13) take the form

$$\begin{aligned} \psi_1 &= \frac{\beta_1 T_o}{(\lambda_1^2 - m^2)} \left\{ \frac{\cosh[\lambda_1(y-a_1)]}{\cosh[\lambda_1 a_1]} - \frac{\cosh[m(y-a_1)]}{\cosh[ma_1]} \right\} e^{(bt+jmx)} \\ \psi_2 &= \frac{\beta_2 T_o}{(\lambda_2^2 - m^2)} \left\{ \frac{\sinh[\lambda_2(y+a_2)]}{\sinh[\lambda_2 a_2]} - \frac{\sinh[m(y+a_2)]}{\sinh[ma_2]} \right\} e^{(bt+jmx)}, \end{aligned} \quad (23)$$

whilst the Green and Zerna potentials introduced in Eq. (16) are given by

$$\begin{aligned} \phi_1 &= C_1 \frac{\cosh[m(y-a_1)]}{\cosh[ma_1]} e^{jmx}; & \phi_2 &= C_2 \frac{\sinh[m(y+a_2)]}{\sinh[ma_2]} e^{jmx} \\ \psi_1 &= D_1 \frac{\sinh[m(y-a_1)]}{\sinh[ma_1]} e^{jmx}; & \psi_2 &= D_2 \frac{\cosh[m(y+a_2)]}{\cosh[ma_2]} e^{jmx}. \end{aligned} \quad (24)$$

The potential functions (23) and (24) are substituted in (15), hence the displacements and stresses over the planes of symmetry and at the friction interface are evaluated. Subsequently, the system (17) is solved for the constants  $C_1$ ,  $C_2$ ,  $D_1$ , and  $D_2$ , and the interface pressure amplitude  $p_o$  is determined from equation (18). Finally, the governing characteristic equation  $f(V, c_1, c_2) = 0$  is given by (21).

By substituting  $c_2 = c_1 - V$ , the problem is reduced to solve the real part ( $f_{Re}(V, c_1) = 0$ ) and the imaginary part ( $f_{Im}(V, c_1) = 0$ ) of the characteristic equation for  $V$  and  $c_1$ . Since there are no accurate and general methods to solve systems of non-linear equations,

a custom made algorithm has been used. Firstly, the wave number  $m$  is fixed and an initial value  $V^{(1)}$  for  $V$  is guessed, thus the real part of the characteristic equation is solved for  $c_1$

$$f_{\text{Re}}(V^{(1)}, c_1) = 0 \quad (25)$$

using a built in Mathematica algorithm, giving  $c_1^{(1)}$ . Subsequently, the imaginary part of the characteristic equation is evaluated at  $(V^{(1)}, c_1^{(1)})$  giving

$$f_{\text{Im}}(V^{(1)}, c_1^{(1)}) = F_{\text{Im}} \quad (26)$$

If  $F_{\text{Im}}$  is different from zero, the above procedure is restarted with a new value for  $V$ . The function  $f_{\text{Im}}(V^{(1)}, c_1^{(1)})$  varies smoothly and continuously, thus a classical bisection method is employed to converge to  $F_{\text{Im}}=0$ , for which the actual critical speed  $V$  and migration speed  $c_1$  are determined.

Moreover, the code has to take account of the fact that the migration speed can take up positive, negative and zero values, thus the definition of  $\xi_i$  and  $\eta_i$  in (6) has to be adjusted as from Appendix, to avoid branch cut problems.

### 3 Results

The general procedure described above is employed to study the propensity towards thermoelastic instability in multi-disk clutches and brakes. Firstly, the effect of the thickness ratio and type of boundary conditions (b.c.) on hot spot formation is investigated. Subsequently, the two-dimensional model is used to determine the onset of instability in a real multi-disk clutch and a comparison with a three-dimensional axisymmetric FE model is performed.

**The Effect of the Thickness Ratio.** The effect of the thickness ratio  $a_1/a_2$  on the critical speed, critical wave parameter and migration speed of the good conductor is analyzed. In order to give general results, the sliding speed is normalized with respect to the product  $k_2 a_2$  and the wave parameter  $ma_2$  is introduced. Common materials for brakes and clutches are considered, as from Table 1. Generally, gray cast iron is employed for metal disks, whilst different materials can be used for the friction linings, namely *non asbestos organic* (NAO), *semi-metallic* (SM), and *hybrid materials* which combine formulations and properties of NAO and SM. The following results are for a NAO material, which is more susceptible to TEI [2].

In Fig. 2, the variation of the critical dimensionless speed with the wave parameter is shown for different values of the thickness ratio  $a_1/a_2$  and the limiting cases of Burton (two half-planes model) and Lee and Barber ( $a_1/a_2 \rightarrow \infty$ ) are presented for comparison. It clearly appears that the Burton's solution is approached only for sufficiently large wave parameters, depending on the thickness ratio  $a_1/a_2$ : the smaller the thickness ratio  $a_1/a_2$  the larger the wave parameter  $ma_2$ . This result can be easily explained noting that as the wave number  $ma_2$  increases, that is shorter wave lengths are considered, the temperature and pressure disturbances penetrates only slightly into the layers affecting a shallow area beneath the surface. Thus for sufficiently large  $ma_2$ , the layers are seen as half-planes by the disturbances, thus Burton's approximation holds true.

At fixed thickness ratio  $a_1/a_2$ , as the wave parameter decreases, the dimensionless critical speed reduces, reaches a mini-

Table 1 Material properties

Material	$E$	$\nu$	$K$	$k$	$\alpha$
	$N/m^2 \times 10^9$		$W/(m^2C)$	$m^2/s \times 10^{-6}$	$^{\circ}C^{-1} \times 10^{-6}$
Gray Cast iron	125	0.25	54	12.98	12
NAO	0.53	0.25	0.5	0.269	30

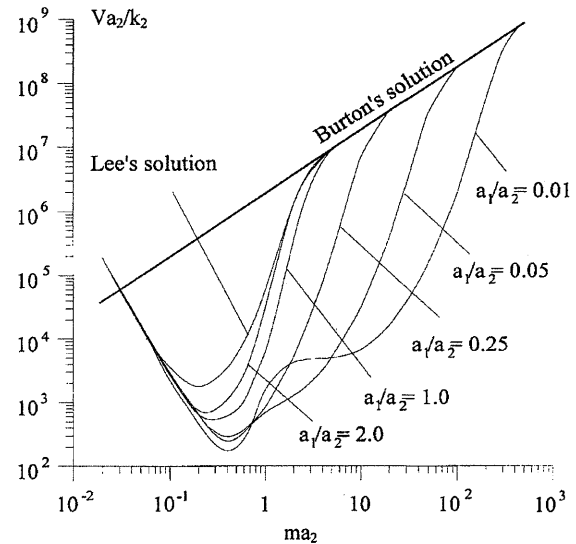


Fig. 2 The effect of the thickness ratio  $a_1/a_2$  on the relationship between critical speed  $V$  and wave number  $m$ , for the dominant mode  $sym_1 - asym_2$

mum and then grows again, showing a characteristic *vee* shape. In addition, at fixed  $ma_2$ , a reduction in thickness ratio leads to a decrease in critical speed. The results plotted in Fig. 2 are for the  $sym_1 - asym_2$  mode, which is the dominant mode, as later discussed.

In the second paragraph, it has been pointed out that an arbitrary perturbation is unstable if at least one of its components is unstable. Generally speaking, the system is driven unstable by the component with wave parameter  $(ma_2)_{\text{min}}$  corresponding to the absolute minimum critical speed  $(Va_2/k_2)_{\text{min}}$ . Therefore, it is important to analyze in detail the effect of the thickness ratio on  $(Va_2/k_2)_{\text{min}}$  and  $(ma_2)_{\text{min}}$ . This is shown in Fig. 3. For sufficiently large thickness ratio, namely  $a_1/a_2 > 10$ , the minimum critical speed and the wave parameter are almost constant and Lee's approximation holds. However, as  $a_1/a_2$  reduces,

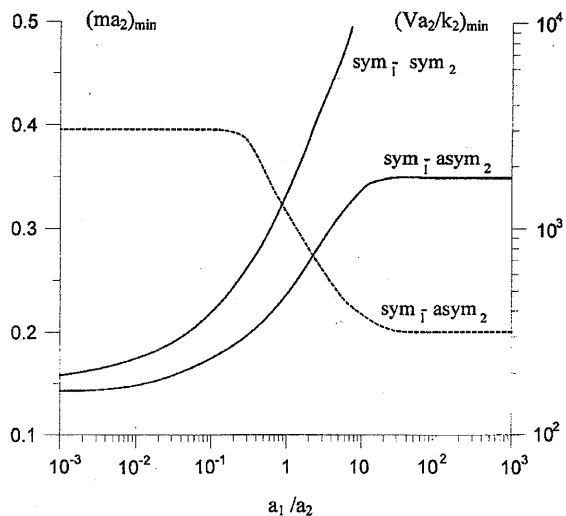


Fig. 3 The effect of the thickness ratio  $a_2/a_1$  on the minimum critical speed  $V$  (solid line) and the wave number  $m$  (dashed line)

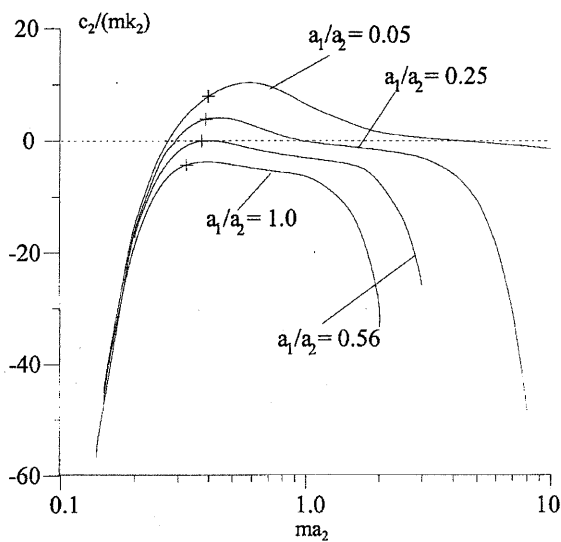


Fig. 4 The effect of the thickness ratio  $a_1/a_2$  on the migration  $c_2$  speed of the good conducting layer

$(Va_2/k_2)_{\min}$  decreases and  $(ma_2)_{\min}$  increases significantly: for common thickness ratio ( $0.1 < a_1/a_2 < 1$ ) a difference of about 80 percent is measured with respect to the Lee and Barber's model. Continuing in decreasing the thickness ratio, both  $(Va_2/k_2)_{\min}$  and  $(ma_2)_{\min}$  tend to distinct fixed values, depending on the material properties. In Fig. 3, it is also shown a comparison between the minimum critical speed for the  $sym_1-asm_2$  and  $sym_1-sym_2$  modes: the former is more critical than the later. Curves for the other two possible modes  $asym_1-sym_2$  and  $asym_1-asym_2$ , which are not included here, have been also produced and they resulted always much higher than the  $sym_1-asm_2$  mode, confirming once again that this is the most critical set of boundary conditions. Therefore, the metal disks are likely to de-

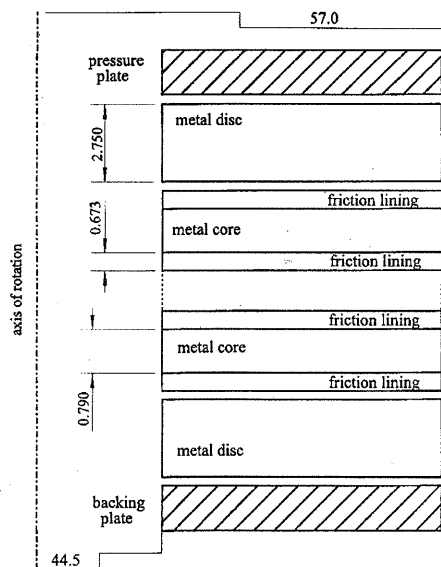


Fig. 5 Geometry and dimensions of a typical multi-disk clutch (all dimensions are expressed in mm)

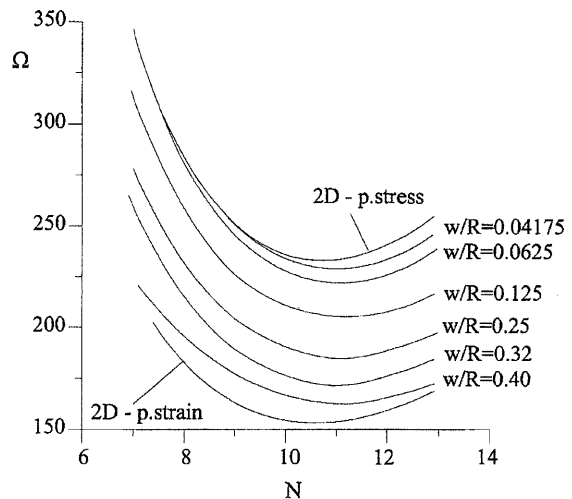


Fig. 6 The relation between the critical rotational speed—the number of hot spots  $N$ , for different radial thickness ratio  $w/R$  of the disks. The two-dimensional solution is obtained for a thickness ratio  $a_1/a_2=0.5$ .

form antisymmetrically, whilst the friction disks are likely to deform symmetrically. So far, the wave parameter  $ma_2$  has been considered as a continuous variable. However, it must be pointed out that in practical applications  $ma_2$  can only take up discrete values and has a minimum. In fact, the pressure perturbation superimposed over the uniform field has to be self-equilibrated meaning that the wave length  $l=2\pi/m$  has to be a submultiple of the mean circumferential length [6], that is

$$ma_2 = N \frac{a_2}{R}, \quad (27)$$

where  $N$  is the integer number of hot spots. In addition to this, it comes up that  $(ma_2)_{\min} = a_2/R$ . Consequently, in order to judge the susceptibility toward hot spotting, it is also worth to investigate the influence of the thickness ratio on the whole curve  $V-m$ . From Fig. 2, it clearly appears that as the thickness ratio reduces the *vee* shape curves are widened, leading to a general reduction in critical speed.

The relationship between the dimensionless migration speed  $c_2^* = c_2/(mk_2)$  and the wave parameter  $ma_2$  is plotted in Fig. 4 for different thickness ratios, namely  $a_1/a_2 = 1.0, 0.56, 0.25, 0.05$ . As the thickness ratio decreases, the curves are shifted toward larger values of the migration speed, and they are widened. From Fig. 4, it appears that for thickness ratios larger than 0.56, the migration speed of the good conducting layer takes up only negative values, whilst for thickness ratios smaller than 0.56,  $c_2^*$  takes up positive and negative values and has two distinct zeros. Notice that  $c_2^* < 0$  means that the perturbation in the poor conductor is faster than the sliding speed ( $c_1 > V$ ); whilst the opposite result holds for  $c_2^* > 0$ . For  $c_2^* = 0$ , the perturbation is stationary with respect to the good conductor. In Fig. 4, the cross marks indicate the locations of the minima for the critical speed.

**The Effect of the Type of Boundary Conditions.** At this point, it is worth to investigate further the inherent nature of the boundary conditions (b.c.), in order to understand why the  $sym_1-asm_2$  mode is dominant. From a mechanical point of view, symmetric b.c. implies zero normal displacements along the layer's mid plane which acts as an infinitely rigid backing plate; whilst antisymmetric b.c. leads to zero normal tractions. There-

**Table 2 Material properties for the real clutch considered**

Material	$E$	$\nu$	$K$	$k$	$\alpha$
	$N/m^2 \times 10^9$		$W/(m^2C)$	$m^2/s \times 10^{-6}$	$^{\circ}C^{-1} \times 10^{-6}$
Metal disk	200	0.30	42	11.91	12
Friction material	0.3	0.12	0.241	0.13	14

fore, a symmetric layer is less compliant than a half-plane, which in turn is less compliant than an antisymmetric layer, that is, introducing fictitious elastic moduli,

$$E_{asym} < E_{half-plane} < E_{sym} \quad (28)$$

By reducing the thickness of the layers, the discrepancies in (28) increase. On the other hand for thermal b.c., a symmetric layer has zero heat flux across its mid-plane, which consequently acts as an insulating panel; whilst the temperature goes to zero on the mid plane of an antisymmetric layer. Therefore, the frictional heat flowing across the thickness of an antisymmetric layer is much larger than that associated to a symmetric layer, meaning that in the first case a fictitious increase in conductivity is measured. It follows that

$$K_{sym} < K_{half-plane} < K_{asym} \quad (29)$$

where again the differences increase as the thickness of the layers reduces.

It has been verified also experimentally [11], that the critical speed of a sliding system is decreased if (i) more rigid and (ii) less conductive friction material, and (iii) more conductive metal disks are used, whilst the variation in elastic modulus of the metal disk has a second order effect on the critical speed, due to the large Young's modulus of steel. Consequently, the dominant mode for a thin metal layer sliding between two friction half-planes (Lee and Barber's model) has to be antisymmetric, since antisymmetric layers are fictitiously more conductive than symmetric layers ( $K_{sym} < K_{asym}$ ). On the contrary, the dominant mode for a thin friction layer sliding between two metal half-planes (Lee and Barber's model with reversed materials) has to be symmetric, since symmetric layers are fictitiously stiffer ( $E_{asym} < E_{sym}$ ) and less conductive ( $K_{sym} < K_{asym}$ ) than antisymmetric layers. This is why the  $sym_1 - asym_2$  case is dominant in the present case. Following similar reasonings, it is also easily explained the reduction in critical speed as the thickness ratio decreases.

**Application to a Real Multi-Disk Clutch.** In this section, the present code is applied to study the propensity toward thermoelastic instability of a real multi-disk clutch and brake, and the results are compared with an accurate three-dimensional FE code [8], which takes into account the effect of axisymmetry and finite radial thickness of the disks. As previously reported, Yi et al. [8] have shown that in multi-disk clutches/brakes the critical speed reduces approaching a fixed minimum value as the number of disks increases, and this minimum is reached for just 9 disks. The material properties employed are listed in Table 2 and the friction coefficient is set equal to  $f=0.13$ .

The geometry of the actual clutch is presented in Fig. 5. Differently from the two dimensional analytical model, the FE code considers composite friction disks made up of a steel core bonded by two friction linings. The first disk of the pack (pressure plate) is affected by a uniform pressure and moves axially thus compressing the disks against the fixed backing plate. In most practical applications, the friction linings are so thick and have such a low conductivity that the thermal boundary layer does not affect the steel core, which than functions as a rigid backing plate. Consequently, the composite friction disk can be replaced by a homogeneous friction layer, with symmetrical boundary conditions, whose half thickness is equal to the actual thickness of the linings. The FE results are thus compared with the present two-

dimensional model with (i)  $sym_1 - asym_2$  boundary conditions and (ii) homogeneous friction layers (Fig. 1), whose half thickness  $a_1$  is equal to the thickness of a real friction lining.

In Fig. 6, the critical rotational speed is plotted against the number of hot spots  $N$  for different values of the radial thickness ratio  $w/R$ , where  $w$  is the difference between the outer and inner radius and  $R$  is the mean radius. The upper line defines the two dimensional plane stress solution and the lower line the two dimensional plane strain solution. In practical applications the radial thickness ratio varies in a relatively small neighbor of  $w/R = 0.25$ . For such commonly used values, it clearly appears from Fig. 6 that the three-dimensional solution is bracketed between the two-dimensional limiting cases and the plane strain assumption can be used for radial thickness ratio  $w/R > 0.2$ , whilst the two-dimensional plane stress approximation can be used for  $w/R < 0.2$ . Also, the shape of the curves and minimum number of hot spots ( $N=11$ ) are not affected by the radial thickness ratio  $w/R$ . Experimental results, reported in [8], have shown that for the present geometrical data and material properties, 12 hot spots were observed on the sliding surfaces of a 5 disk clutch, which is in good agreement with the  $N=11$  estimated by the present analytical formulation.

#### 4 Discussion and Conclusions

In this work, a two dimensional analytical model is proposed to predict the critical sliding speed in multi-disk clutches and brakes. Since the present code considers disks with finite thickness, it has been employed to investigate the effect of the disks' thickness ratio  $a_1/a_2$  on the (i) critical speed, (ii) critical wave parameter, and (iii) migration speed of the sliding system. Firstly, a comparison with previous analytical models has been performed showing that the Lee and Barber's solution, strictly valid for an infinitely thick friction layer ( $a_1 \rightarrow \infty$ ), is approached for sufficiently large thickness ratios ( $a_1/a_2 > 10$ ). Whilst, for ratios commonly used in practice ( $0.1 < a_1/a_2 < 1$ ) the Lee and Barber's model overestimates significantly the critical speed with respect to the present formulation, with a difference in critical speed of about 80 percent. In general, it is found that the critical speed is strongly influenced by the thickness ratio in the neighbor of  $a_1/a_2 = 1$ , which is a value commonly used in practice. Also, it is found that the critical wave parameter increases slightly as the thickness ratio decreases. This means that the susceptibility toward hot spotting not only can be reduced by (i) changing the properties of the friction material, but also by (ii) increasing the thickness of the friction lining, or (iii) reducing the thickness of the metal disk, that is adjusting suitably the thickness ratio  $a_1/a_2$  thus avoiding any additional cost associated with the development of new friction materials.

In addition, the two-dimensional analytical model is employed to estimate the critical rotational speed in a real multi-disk clutch, with 9 or more disks, and the results are compared with a three-dimensional axisymmetric FE code. It is verified that the two-dimensional plane strain solution gives conservative results for the critical speed and can be used for  $w/R < 0.20$ , whilst for  $w/R > 0.20$  the two-dimensional plane stress solution must be used. Also, the critical number of hot spots  $N$  and the shape of the curve is not influenced by the radial thickness ratio and coincide with what predicted by the two-dimensional model.

#### Acknowledgments

The authors would like to express their appreciation for the continuous support given by Prof. J. R. Barber of the University of Michigan. Dr. P. Zagrodzki, at the Raybestos Products Company, should also be acknowledged for the useful discussions, and Mr. Yun-Bo Yi, at the University of Michigan, for helping in using the FE code.

## Nomenclature

$a_i$  = thickness of the disk  $i$   
 $R$  = mean radius of the disks  
 $w$  = radial thickness of the disks  
 $m$  = wave number of the perturbation  
 $b$  = growth rate of the perturbation  
 $c$  = absolute velocity of the perturbation  
 $c_i$  = migration speed of the perturbation  
 $x$  = coordinate in the  $x$ -direction moving with the perturbation  
 $x_i$  = local coordinate in  $x$ -direction stationary in body  $i$   
 $y$  = coordinate in the  $y$ -direction moving with the perturbation  
 $y_i$  = local coordinate in  $y$ -direction stationary in body  $i$   
 $V$  = sliding speed  
 $c_p$  = specific heat  
 $E$  = elastic modulus  
 $f$  = coefficient of friction  
 $j$  = imaginary unity  
 $K$  = thermal conductivity  
 $k$  = thermal diffusivity  
 $\alpha$  = coefficient of thermal expansion  
 $\mu$  = shear modulus  
 $\nu$  = Poisson's ratio  
 $\rho$  = density  
 $\sigma$  = stress  
 $p$  = pressure  
 $T$  = temperature  
 $u$  = displacement  
 $q$  = heat flux  
 $\phi$  = potential function  $A$  [9]  
 $\omega$  = potential function  $D$  [9]  
 $\psi$  = strain potential

## Appendix

Since the migration speed  $c_i$  can assume either positive, zero or negative values, the definition of  $\lambda_i$  deserves special attention. Putting  $b=0$ , from (6), it follows that

$$\lambda_i = \xi_i + j \eta_i = \sqrt{m^2 - j \left( \frac{m c_i}{k_i} \right)} = \pm \sqrt{r} \left[ \cos \frac{\theta}{2} + j \sin \frac{\theta}{2} \right], \quad (30)$$

where

$$r = \sqrt{m^4 + \left( \frac{m c_i}{k_i} \right)^2}; \quad \theta = \arctan \left( - \frac{c_i}{m k_i} \right). \quad (31)$$

Substituting (30) in (31) and using classical trigonometrical formulas for  $\cos \theta/2$  and  $\sin \theta/2$ , the following four different cases are individuated,

$$(a) \quad \lambda_i = \xi_i + j \eta_i = + \sqrt{\frac{m^2+r}{2}} - j \sqrt{\frac{-m^2+r}{2}};$$

$$c_i < 0 \quad \text{and} \quad \left| \frac{c_i}{m k_i} \right| > 1$$

$$(b) \quad \lambda_i = \xi_i + j \eta_i = + \sqrt{\frac{m^2+r}{2}} + j \sqrt{\frac{-m^2+r}{2}};$$

$$c_i < 0 \quad \text{and} \quad \left| \frac{c_i}{m k_i} \right| \leq 1$$

$$(c) \quad \lambda_i = \xi_i + j \eta_i = + \sqrt{\frac{m^2+r}{2}} - j \sqrt{\frac{-m^2+r}{2}};$$

$$c_i > 0 \quad \text{and} \quad \frac{c_i}{m k_i} < 1$$

$$(d) \quad \lambda_i = \xi_i + j \eta_i = + \sqrt{\frac{m^2+r}{2}} + j \sqrt{\frac{-m^2+r}{2}};$$

$$c_i > 0 \quad \text{and} \quad \frac{c_i}{m k_i} \geq 1,$$

where  $\xi_i$  has to be always positive, because the perturbation amplitude has to decay away from the friction interface. For  $c_i=0$  ( $\lambda_i=m$ ), the definition (13) has to be changed with (14).

## References

- [1] Barber, J. R., 1969, "Thermoelastic Instability in the Sliding of Conforming Solids," *Proc. R. Soc. London, Ser. A*, **312**, pp. 381-394.
- [2] Smales, H., 1994, "Friction materials-black art or science?," *Proc. Inst. Mech. Eng.*, **209**, pp. 151-157.
- [3] Yang, Y., Twaddell, P. S., Chen, Y. F., and Lam, R. C., 1997, "Theoretical and Experimental Studies on the Thermal Degradation of Wet Friction Materials," SAE Paper 970978.
- [4] Takezaki, K., and Kubota, M., 1992, "Thermal and Mechanical Damage of Paper Wet Friction Material Induced by Non-Uniform Contact," SAE Paper 922095.
- [5] Burton, R. A., Nerlikar, V., and Kiliparti, S. R., 1972, "Thermoelastic Instability in Seal-Like Configuration," *Wear*, **24**, pp. 177-188.
- [6] Lee, K., and Barber, J. R., 1993, "Frictionally Excited Thermoelastic Instability in Automotive Disk Brakes," *ASME J. Tribol.*, **115**, pp. 607-614.
- [7] Zagrodzki, P., 1990, "Analysis of Thermomechanical Phenomena in Multi-Disk Clutches and Brakes," *Wear*, **140**, pp. 291-308.
- [8] Yi, Y. B., Barber, J. R., and Zagrodzki, P., 1999, "Eigenvalue Solution of Thermoelastic Instability Problems Using Fourier Reduction," accepted by the *Proc. R. Soc. London*.
- [9] Green, A. E., and Zerna, W., 1968, *Theoretical Elasticity*, Oxford University Press, Oxford.
- [10] *Mathematica: A System for Doing Mathematics by Computer, II* 1992, Addison-Wesley, Redwood City, California.
- [11] Anderson, A. E., and Knapp, R. A., 1990, "Hot Spotting in Automotive Friction Systems," *Wear*, **138**, pp. 319-337.